Journal of Chromatography A, 1226 (2012) 43–47

Contents lists available at ScienceDirect

Journal of Chromatography A

journal homepage: www.elsevier.com/locate/chroma

Photodeposited silver nanoparticles for on-column surface-enhanced Raman spectrometry detection in capillary electrophoresis

Jan Přikryl, Karel Klepárník*, František Foret

Institute of Analytical Chemistry of the Academy of Sciences of the Czech Republic, Brno, Czech Republic

ARTICLE INFO

Article history:
Available online 22 July 2011

Keywords:
SERS
Capillary electrophoresis
Photodeposition
Metal nanoparticle

ABSTRACT

A new, simple photo-deposition method of silver nanoparticles induced by laser inside a fused-silica capillary is described and tested. Silver nanoparticles are immobilized using Ar-ion laser beam of a wavelength of 488 nm and power of 3.6 mW for 60 min. The photodeposited compact spot of a size of ~10 μm is temporary and spatially stable and resistant to a hydrodynamic flow. The deposit has very good properties for surface-enhanced Raman scattering and serves well for detection in capillary electrophoresis. The advantage of this approach is that neither the silver nanoparticles nor the chemicals for their preparation are components of the background electrolyte during the electrophoretic separation. Thus, the substrate formation and separation of analytes are two independent processes and can be performed under their optimum conditions. The zone broadening due to the sorption of analytes on the immobilized nanoparticles can be significantly reduced by an addition of 20% solution of methanol. The efficiency of capillary electrophoresis and detection selectivity of surface-enhanced Raman scattering induced by He–Ne laser at 632.8 nm is demonstrated by the 3D electropherograms of rhodamines 123 and B as model samples. The limits of detection of about 49 and 150 fmol (1 and 2 μM) have been reached for rhodamine B and 123, respectively.

1. Introduction

The discovery of surface-enhanced Raman scattering (SERS) has revealed its great potential not only in analytical chemistry but also in biology, pharmacy, environmental chemistry, biomedicine, etc. Although the first SERS experiment with pyridine adsorbed on an electrochemically roughened silver electrode was performed by Fleischmann et al. as early as in 1974 [1], SERS mechanism has not been completely explained yet. The method is based on coupled optical responses of nanostructured metals and analyte molecules in a close proximity [2]. According to the electromagnetic theory, the laser induced plasmon enhances electric field strength at metal surfaces inducing structure-specific Raman scattering on molecules in the proximity to such a metal surface (e.g., adsorbed due to physical forces). However, many experiments proved also chemical mechanism of the enhancement [3,4]. The theory of the chemical mechanism, which does not involve the surface plasmon, is based on the charge transfer within the complex between a metal particle and chemisorbed molecule. Currently, SERS has the status of a well established analytical spectrometric method providing highly sensitive quantitative [5–8] and qualitative analyses [9]. The vibration frequencies of an analyte affect the spectrum of the scattered light, which is used for the analyte identification. This is based on the detection of characteristic bands of functional groups or the fingerprint region of the vibration spectra. Thus, a high specificity and sensitivity of this method makes SERS a highly applicable analytical method. Even single molecule (SM) sensitivity of SERS was proposed by Nie and Kneipp [10,11] theoretically and, several years later, SM sensitivity of SERS has been experimentally proved by various techniques [12–19]. Many publications describe various SERS applications such as protein detection [4,20], SERS imaging of living cells [4,21], cancer diagnostics [22], glucose sensing or SERS immunoassays [4].

In most of the applications mentioned above, SERS was used as a stand-alone method. However, relatively little attention was focused to coupling of SERS with separation methods such as liquid chromatography [23–26] or capillary electrophoresis (CE). In 2000, Nirode et al. published a simple way to integrate the on-column SERS detection in CE by usage of SERS-active silver nanoparticles (Ag NPs) suspended in the CE background electrolyte (BGE) [27]. They reported limits of detection (LOD) of 1 μM and low-nanomolar for riboflavin and rhodamine 6G (Rh6G), respectively. However, the SERS spectra degraded with time, probably due to the sorption of nanoparticles on the capillary wall. Moreover, the influence of NPs on the separation efficiency was not discussed in detail. Recently, the research in the field of coupling CE and SERS was focused on

* Corresponding author. Tel.: +420 532 290 122; fax: +420 541 212 113.
E-mail address: kleparnik@iach.cz (K. Klepárník).

0021-9673/$ – see front matter © 2011 Elsevier B.V. All rights reserved.
doi:10.1016/j.chroma.2011.07.045

the off-line approach. In this arrangement, the CE effluent was deposited on a moving substrate with a metal nanostructure on the surface [28–31]. The substrate moved close to the end of the separation capillary and the effluent was deposited by cohesive forces of surface tension. In these off-line approaches various substrates, such as Ag NPs [28,29], Ag coated Au NPs [29] or sputtered Ag film [29] deposited on a roughened glass microscope slide; etched silver foil [30], quartz plate with vapor-deposited thin silver film [30], silver oxalate-coated silica TLC plate [30,32] or silica TLC plate with deposited citrate-, borate-reduced or gold-coated Ag NPs, were used. Recently, the on-column SERS detection on in situ prepared silver substrate was published [33]. In this paper, a spot of SERS substrate was prepared by laser-induced citrate reduction of silver nitrate during the CE separation. A detection of 0.25–25 ppm Rh6G and Cu complex of 4-(2-pyridylazo)resorcinol at a laser power of 1.4–3.6 mW and an acquisition time of 5 s was presented. The authors declare that the main advantage of this detection approach is no memory effect due to a small area of the silver substrate.

The photo-induced aggregation of gold NPs from their free suspensions in organic solvents was published by Kimura et al. [34,35] and Niidome et al. [36,37]. A photo-induced deposition of silver NPs on fused-silica in water has not been described, yet. Several papers describe principles and applications of fixation of gold [38,39] or silver [40] NPs on polyimide or glass substrates. In these methods, suspension of NPs is inkjet printed on a substrate and then this nanostructured micropattern is sintered by laser irradiation. Laser sintering of silver NPs, an alternative to thermal sintering, is allowed by their lower melting temperature (approx. 150 °C), when compared to bulk silver (960 °C) [41]. This method, however, has been used exclusively in microelectronics.

The objective of this paper is the demonstration of the laser-induced photodeposition of a stable silver nanoparticle deposit on an inner wall of a fused-silica capillary. The photodeposited Ag NPs serve as an enhancement element of Raman scattering in the detection window of CE. The advantage of this approach is the independence of the nanoparticle deposit preparation step on the separation process. The electromigration of analytes is not influenced by interactions with a metal colloid or chemicals used for its formation. Based on the theory of SERS, the close contact of analytes with nanostructured metal surfaces is fundamental for signal enhancement. On the other hand, slow sorption kinetics on the Ag deposit can cause zone broadening in CE; however, this can be minimized by chemical modification of the BGE. Under optimized conditions, a 3D record of the CE separation with SERS detection can provide a quantitative analysis of separated components as well as their identification.

2. Materials and methods

2.1. Reagents

Silver nitrate (min. 99.8%), tri-sodium citrate dihydrate (min. 99%) and hydrochloric acid (35%, G.R.) were purchased from Lach-Ner, Czech Republic. 3-[Cyclohexylamino]-1-propanesulfonic acid (CAPS), *N*-tris[hydroxymethyl]methyl-3-aminopropanesulfonic acid (TAPS, min. 99.5%), rhodamine 123 (Rh123, min. 90.0%), Rh6G (99%) were obtained from Sigma–Aldrich, Switzerland, methanol (min. 99.8%) from Scharlau, Spain and tris(hydroxymethyl)aminomethane (TRIS, min. 99.8%) from AMRESCO Inc., USA. Rhodamine B (RhB) was purchased from Lachema Brno, Czech Republic. All reagents were used as received. Aqueous solutions were prepared using deionized water purified by reverse osmosis (Neptune, Purite Ltd., United Kingdom).

2.2. Photodeposition

Colloidal Ag nanoparticles were prepared by Lee&Meisel citrate procedure [42] and the absorption spectrum of the resulting brownish suspension was characterized by typical absorption maximum ~412 nm and FWHM ~115 nm. For the photodeposition of Ag NPs, crude silver colloid was decanted (14,100 × *g*; 8 min) and the sediment was resuspended in 50 mM CAPS (pH 10.0). The final concentration of Ag NPs was 3.6 mg ml^{-1}. Photodeposition was performed in the detection window of the fused-silica capillary (Polymicro Technologies, USA) by irradiation with Ar-ion laser (LGK 7872 ML, LASOS Lasertechnik GmbH, Germany) at 488 nm. The laser light was focused after passing through the laser line filter (488 nm, Oriel) by biconvex lens (focal length = 18 mm) on the inner wall of capillary (I.D. 50 μm, O.D. 375 μm). The laser power after the passage through all optical elements was set to 3.6 mW (monitored by NOVA II, OPHIR Laser Measurement Group, Israel).

Before the photodeposition, the capillary was rinsed with 1 M NaOH followed by 1 M HCl, water and 50 mM CAPS (pH 10.0) (each rinse for 15 min, 6.67 μl min^{-1}). After the capillary pretreatment, Ag NPs were photodeposited for a 60 min under the continual flow (1.67 μl min^{-1}) of NPs suspension prepared according to the procedure mentioned above. After the photodeposition, the capillary was rinsed with water (for 1 min, 1.67 μl min^{-1}).

2.3. CZE with SERS detection

Raman-active compounds were electrokinetically introduced to a bare fused-silica capillary (I.D. 50 μm, O.D. 375 μm, effective length 15 cm, total length 25 cm) and separated at a positive voltage applied to the injection end by power source Spellman CZE 1000 (Plainview, NY, USA). Under these conditions, the electroosmotic flow (EOF) carried all negatively charged analytes to the detection window with photodeposited Ag NPs. The EOF mobility was determined to be of 23×10^{-9} m^2 V^{-1} s^{-1}. The laboratory-built Raman detection system consisted of an epifluorescence microscope body (JENALUMAR, Carl Zeiss Jena, Germany) equipped with a 50× (0.95 NA) microscope objective and a He–Ne laser (632.8 nm, 15 mW). The epi-illumination through the microscope objective was used to induce the Raman scattering, which was collected by the same objective and passed through a dichromatic mirror and Raman notch filter. The scattered light was then analyzed by a spectrograph (Shamrock SR-303i, Andor, UK) equipped with a diffraction grating (600 l/mm, blazed for 500 nm) and collected by a 16-bit deep cooled (−90 °C) back-illuminated CCD camera (iDus DU420A BR-DD, Andor, UK). The fluorescence background of all measured SERS spectra was corrected using an intelligent background-correction algorithm for highly fluorescent samples in Raman spectrometry and using a free software environment for statistical computing and graphics R (version 2.8.1) [43].

3. Results and discussion

3.1. Dependence of SERS signal on Ag NPs concentration

The SERS spectrum of 1×10^{-6} M Rh6G and the dependence of its intensity on the concentration of Ag NPs suspension are shown in Fig. 1. The typical narrow vibration bands are favorable for a high-resolution qualitative analysis. The individual bands are not detected in the absence of the colloid. The signal intensity increases with increasing the concentration of Ag NPs. Nevertheless, the concentration cannot be increased without limits. For applications of SERS in separation methods, the optimization of colloid concentration is always a trade-off between the signal maximization and minimization of long term interactions with

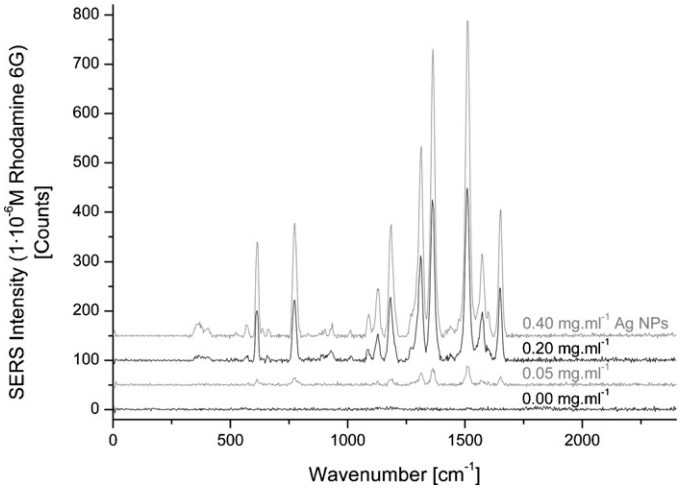

Fig. 1. Dependence of SERS signal of 1×10^{-6} M Rh6G on the Ag NPs concentration varying from 0 to 0.40 mg ml^{-1} (displayed with offsets of 0, 50, 100 and 150 Counts, respectively). Aggregating buffer 10 mM TRIS/TAPS, pH 8.3. Collection time 500 ms.

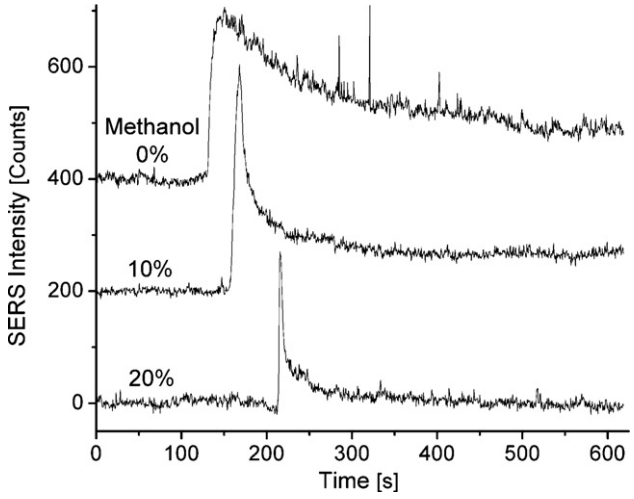

Fig. 3. Dependence of spreading of Rh6G electrophoretic zones on concentration of methanol (0%, 10%, 20%) added to BGE. Records displayed with SERS intensity offsets. Detection of SERS signal at 1514 cm^{-1} vibrational band. Electrokinetic injection from 1×10^{-6} M solution of Rh6G in 40 mM CAPS at 6 kV for 10 s. Electrophoresis in 50 mM CAPS, pH 10, at 6 kV.

analytes. This is especially critical when the colloid is suspended in the BGE and can negatively affect the separation resolution. In this respect, the presence of enhancement elements only at the detection window brings a substantial advantage.

3.2. Deposition and deposit stability

During the SERS measurement in the background electrolyte containing the Ag nanoparticles, we have observed a continual increase of the signal as well as the scatter of the laser light around the capillary. A thorough inspection of this phenomena revealed that this increase was caused by the laser-induced deposition of Ag NPs on the capillary wall. Therefore, we have studied the photodeposition and shape of the deposit at increasing laser powers of 3.6 mW, 18.3 mW and 36.3 mW. In general, the area and volume of the deposit increase with the laser power. The test of a resistance to hydrodynamic flow at the range of flow rates from 0.17 μl min^{-1} (mean linear velocity 1.4 mm s^{-1}) to 10.6 μl min^{-1} (90.0 mm s^{-1}) proved a satisfactory stability of the spot formed at the lowest laser power of 3.6 mW (Fig. 2). The spot of size of ~10 μm was reproducibly photodeposited by an Ar-ion laser. The estimated diameter of the laser Gaussian beam after the passage through the lens of a focal length of 18 mm was~7.5 μm. Larger deposits were not compact and were easily removed at a flow rate of mere 0.17 μl min^{-1}. The typical microphotography of the immobilized Ag NPs on the irradiated spots of the capillary inner wall is shown in Fig. 2.

The irradiation by lower energy He–Ne laser (632.8 nm) does not result in formation of Ag NPs photodeposits. The probable reason is that 488 nm line could excite surface plasmon on silver nanoparticles more effectively, whereas the 632.8 nm He–Ne laser line is outside the surface plasmon region. Since we did not study these phenomena in detail, we can only speculate that a local overheating is responsible for the sintering. Although, the process of sintering of the Ag NPs was observed by scanning electron microscopy at a temperature of 150 °C [41], it is possible that the particle surface premelting starts at a lower temperature.

3.3. Optimization of the electrophoretic conditions

A close contact of analytes with the surface of the substrate plays a key role in SERS applications. Thus, sorption of analytes on the substrate surface can improve the SERS signal; however, a slow or irreversible sorption deteriorates the separation resolution. In our case, when the SERS substrate is formed prior to the separation, the concentration and composition of BGE can be optimized regardless of conditions needed for the substrate formation.

The sorption on the silver surface can be reduced by methanol, a better solvent for rhodamines than water. The effect of methanol added into BGE on the peak tailing is shown in Fig. 3. The narrow zone of Rh6G obtained in BGE with 20% of methanol (Fig. 3) demonstrates its positive effect. More pronounced peak tailing and the unequal level of baseline signal behind the peaks at lower methanol concentrations confirm slow or even irreversible sorption of Rh6G on the SERS substrate. Therefore, 20% of methanol was added into

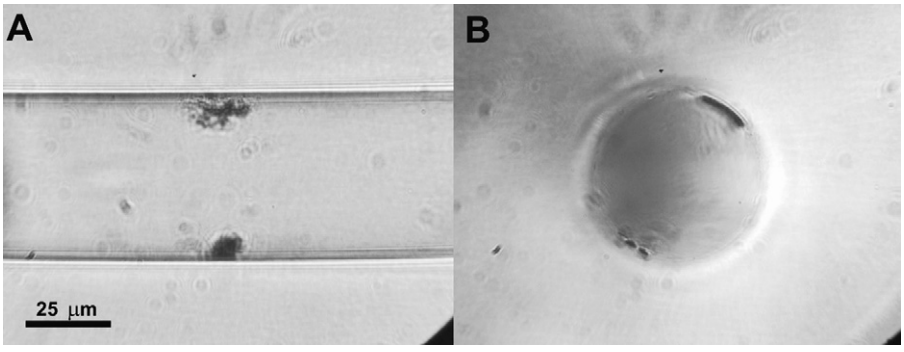

Fig. 2. Microphotograph of Ag NPs deposited inside the fused-silica capillary (I.D. 50 μm) by irradiation with Ar-ion laser (488 nm, 3.6 mW) for 60 min. Magnification 22×. Side view (A), axial view (B).

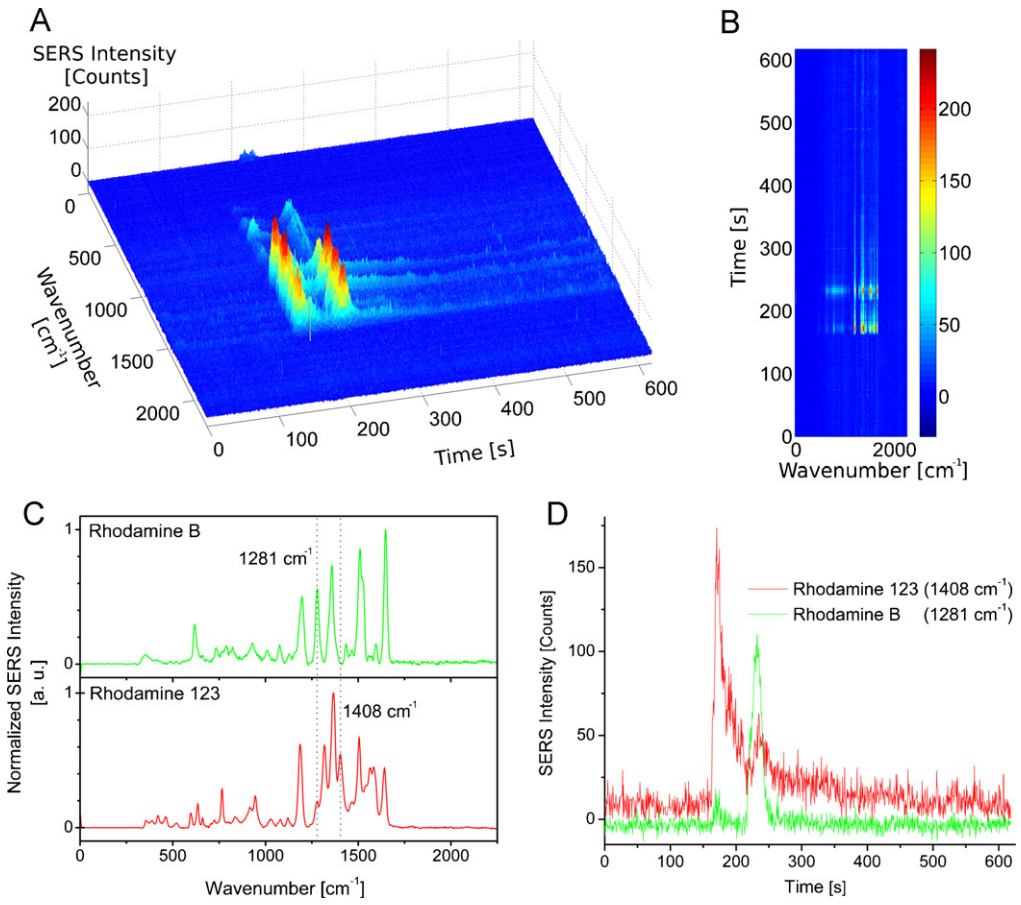

Fig. 4. (A) CZE–SERS 3D electropherogram and (B) SERS intensity map of separation of analytes Rh123 and RhB (electrokinetic injection: 10 s, 12 kV from 5×10^{-5} M Rh123, 2.5×10^{-5} M RhB, 10% methanol, 20 mM CAPS, pH 10; separation: 40 mM CAPS, 20% methanol, pH 10, 6 kV; collection time of 500 ms). (C) Normalized SERS spectra of Rh123 and RhB measured in steady-state mode with Ag NPs. (D) CZE–SERS electropherograms of Rh123 and RhB extracted from 3D record at their specific vibrational bands (Rh123 – 1408 cm^{-1} and RhB – 1281 cm^{-1}).

the BGE for the separation of Rh123 and RhB to ensure a fast and reversible sorption of rhodamines on the SERS substrate. A slight increase of the migration time was caused mainly by changes in electrical permitivity and viscosity of BGEs with different methanol concentrations, and therefore by reduced EOF inside the capillary.

3.4. CZE separation of rhodamines with SERS detection

On-column SERS detection of CZE of rhodamines Rh123 and RhB is demonstrated as a 3D record in Fig. 4A and B. Here, the Raman scattering of the 632.8 nm HeNe laser radiation was analyzed by the spectrograph and detected by CCD camera. The SERS spectra were detected with a collection time of 500 ms. The collection time was chosen as a compromise between good detection sensitivity and resolution of electropherograms. The electrophoretic zone of Rh123 (171 s) exhibits main SERS bands at 597 cm^{-1}, 636 cm^{-1}, 766 cm^{-1}, 1186 cm^{-1}, 1322 cm^{-1}, 1369 cm^{-1}, 1408 cm^{-1}, 1505 cm^{-1}, 1590 cm^{-1}, 1643 cm^{-1}, whereas the zone of RhB (232 s) at 621 cm^{-1}, 1186 cm^{-1}, 1281 cm^{-1}, 1358 cm^{-1}, 1505 cm^{-1}, 1646 cm^{-1}. These SERS spectra, enhanced on a photodeposited Ag substrate, are in good agreement with those already reported in the literature [44–46] and measured in a steady-state mode with suspension of colloidal Ag NPs (Fig. 4C).

To demonstrate the separation recorded at the characteristic vibrational bands of Rh123 and RhB, the wavenumbers of 1408 cm^{-1} and 1281 cm^{-1} were chosen, as shown in Fig. 4C. Both records in Fig. 4D taken at the specific wavenumbers demonstrate the separation. The LODs of 49 and 150 fmol (1 and 2 μM) have been reached for RhB and Rh123, respectively. Our LOD for rhodamine 6G was 1 fmol (70 nM) what is comparable with the results of Nirode et al. [27] who declare a low nanomolar LOD. The LOD was evaluated as the original concentration of an injected analyte giving the electrophoretic peak signal 3 times higher than the standard deviation of the baseline short time noise. This evaluation, which is not generally correct for electromigrational methods, is acceptable here, since the sample was dissolved in 2 times diluted BGE used in electrophoresis. Hence, no predominant stacking phenomena can be expected to bias the LOD. Under this condition, the average detector signal can approximately be regarded as the response to the concentration of injected sample.

4. Conclusions

A new method for the preparation of stable photodeposits of Ag nanoparticles on inner surface of fused-silica capillaries is described. The photodeposited cluster of particles in the detection window of a separation capillary is used as a substrate for SERS detection, which provides the quantitative as well as qualitative analysis of separated components in a certain range of concentrations. The sensitivity of the method is based on the enhancement factor, which can reach values of over 10^{10} for some substances [4]. Under these circumstances, SERS becomes a potential alternative to fluorescence detection with the benefit of the qualitative information without labeling. The advantages of this simple procedure for the substrate preparation, when compared with previously published methods, are two mutually independent steps: (i) on-column

photodeposition of SERS substrate and (ii) CE separation in free BGE without additives needed for the deposition. Thus, both steps can be controlled and optimized independently. The irradiation by Ar-ion laser beam (wavelength of 488 nm, power of 3.6 mW) focused on the middle of the capillary for 60 min proved to be optimum for the preparation of compact Ag NPs spot. The photodeposit of about 10 μm in diameter formed inside the capillary was resistant to the flow rate as high as 10.6 μl min^{-1}, i.e. at a mean linear velocity of 90 mm s^{-1} in a capillary of 50 μm I.D. The detection on the SERS substrate was tested by the separation of rhodamines Rh123 and RhB as model samples in 40 mM CAPS with an addition of methanol to reduce sorption of the analytes. In SERS applications, a close contact of analytes with surface of the substrate plays a crucial role. On the other hand, analyte adsorption on the SERS substrate may deteriorate the separation resolution. The positive effect of methanol concentration on the reduction of electrophoretic peak widths was proved. At a 20% concentration of methanol, peak widths were reduced substantially, while the detection signal was preserved. In addition to possible analytical applications, CE with SERS detection could be a suitable tool for the investigation of SERS phenomena due to the advantage of high-throughput measurements, amenability to automation and low consumption of chemicals.

Acknowledgements

The research was financially supported by Grants of the Grant Agency of the Czech Republic 203/08/1680, P301/11/2055, the Ministry of Education, Youth and Sports # LC06023 and Research Plan of the Institute of Analytical Chemistry ASCR, v.v.i. – provider's code AV0, identification code Z40310501.

References

[1] M. Fleischmann, P.J. Hendra, A.J. McQuillan, Chem. Phys. Lett. 26 (1974) 163.
[2] M. Moskovits, Rev. Mod. Phys. 57 (1985) 783.
[3] A. Campion, P. Kambhampati, Chem. Soc. Rev. 27 (1998) 241.
[4] K. Kneipp, M. Moskovits, H. Kneipp (Eds.), Surface-Enhanced Raman Scattering: Physics and Applications, Springer-Verlag GmbH, Berlin, 2006.
[5] D.L. Stokes, T. Vo-Dinh, Sens. Actuators, B 69 (2000) 28.
[6] J. Chowdhury, M. Ghosh, P. Pal, T.N. Misra, J. Colloid Interface Sci. 263 (2003) 318.
[7] K.E. Shafer-Peltier, C.L. Haynes, M.R. Glucksberg, R.P. Van Duyne, J. Am. Chem. Soc. 125 (2003) 588.
[8] M. Sackmann, A. Materny, J. Raman Spectrosc. 37 (2006) 305.
[9] G.A. Baker, D.S. Moore, Anal. Bioanal. Chem. 382 (2005) 1751.
[10] S.M. Nie, S.R. Emery, Science 275 (1997) 1102.
[11] K. Kneipp, Y. Wang, H. Kneipp, L.T. Perelman, I. Itzkan, R. Dasari, M.S. Feld, Phys. Rev. Lett. 78 (1997) 1667.
[12] H.X. Xu, E.J. Bjerneld, M. Kall, L. Borjesson, Phys. Rev. Lett. 83 (1999) 4357.
[13] A. Otto, J. Raman Spectrosc. 33 (2002) 593.
[14] E.C. Le Ru, M. Meyer, P.G. Etchegoin, J. Phys. Chem. B 110 (2006) 1944.
[15] P.G. Etchegoin, M. Meyer, E.C. Le Ru, Phys. Chem. Chem. Phys. 9 (2007) 3006.
[16] J.A. Dieringer, R.B. Lettan, K.A. Scheidt, R.P. Van Duyne, J. Am. Chem. Soc. 129 (2007) 16249.
[17] B. Vlckova, M. Moskovits, I. Pavel, K. Siskova, M. Sladkova, M. Slouf, Chem. Phys. Lett. 455 (2008) 131.
[18] M. Sladkova, B. Vlckova, I. Pavel, K. Siskova, M. Slouf, J. Mol. Struct. 924–926 (2009) 567.
[19] P.G. Etchegoin, E.C. Le Ru, Anal. Chem. 82 (2010) 2888.
[20] X.X. Han, B. Zhao, Y. Ozaki, Anal. Bioanal. Chem. 394 (2009) 1719.
[21] S. Schlucker, Chemphyschem 10 (2009) 1344.
[22] Y.S. Huh, A.J. Chung, D. Erickson, Microfluid. Nanofluid. 6 (2009) 285.
[23] R.J. Dijkstra, F. Ariese, C. Gooijer, U.A.Th. Brinkman, TrAC Trends Anal. Chem. 24 (2005) 304.
[24] F. Ni, L. Thomas, T.M. Cotton, Anal. Chem. 61 (1989) 888.
[25] S.A. Soper, K.L. Ratzlaff, T. Kuwana, Anal. Chem. 62 (1990) 1438.
[26] A. Orinak, I. Talian, E.V. Efremov, F. Ariese, R. Oriaakova, Chromatographia 67 (2008) 315.
[27] W.F. Nirode, G.L. Devault, M.J. Sepaniak, Anal. Chem. 72 (2000) 1866.
[28] G.L. DeVault, M.J. Sepaniak, Electrophoresis 22 (2001) 2303.
[29] L. He, M.J. Natan, C.D. Keating, Anal. Chem. 72 (2000) 5348.
[30] R.J. Dijkstra, A. Gerssen, E.V. Efremov, F. Ariese, U.A.Th. Brinkman, C. Gooijer, Anal. Chim. Acta 508 (2004) 127.
[31] D.A. Roman, E. Efremov, F. Ariese, A.S. Carretero, C. Gooijer, Anal. Bioanal. Chem. 382 (2005) 180.
[32] P. Matejka, J. Stavek, K. Volka, B. Schrader, Appl. Spectrosc. 50 (1996) 409.
[33] N. Leopold, B. Lendl, Anal. Bioanal. Chem. 396 (2010) 2341.
[34] N. Satoh, H. Hasegawa, K. Tsujii, K. Kimura, J. Phys. Chem. 98 (1994) 2143.
[35] Y. Takeuchi, T. Ida, K. Kimura, J. Phys. Chem. B 101 (1997) 1322.
[36] Y. Niidome, A. Hori, H. Takahashi, S. Yamada, in: Y. Iwasawa, N. Oyama, H. Kunieda (Eds.), Studies in Surface Science and Catalysis, Elsevier, Tokyo, 2001, pp. 359–362.
[37] Y. Niidome, A. Hori, H. Takahashi, Y. Goto, S. Yamada, Nano Lett. 1 (2001) 365.
[38] N.R. Bieri, J. Chung, S.E. Haferl, D. Poulikakos, C.P. Grigoropoulos, Appl. Phys. Lett. 82 (2003) 3529.
[39] J. Chung, S. Ko, C.P. Grigoropoulos, N.R. Bieri, C. Dockendorf, D. Poulikakos, J. Heat Trans.-T. ASME 127 (2005) 724.
[40] K. Yung, S. Wu, H. Liem, J. Mater. Sci. 44 (2009) 154.
[41] K.S. Moon, H. Dong, R. Maric, S. Pothukuchi, A. Hunt, Y. Li, C.P. Wong, J. Electron. Mater. 34 (2005) 168.
[42] P.C. Lee, D. Meisel, J. Phys. Chem. 86 (1982) 3391.
[43] Z.M. Zhang, S. Chen, Y.Z. Liang, Z.X. Liu, Q.M. Zhang, L.X. Ding, F. Ye, H. Zhou, J. Raman Spectrosc. 41 (2009) 659.
[44] J. Chowdhury, P. Pal, M. Ghosh, T.N. Misra, J. Colloid Interface Sci. 235 (2001) 317.
[45] J. Sarkar, J. Chowdhury, P. Pal, G.B. Talapatra, Vib. Spectrosc. 41 (2006) 90.
[46] J.T. Zhang, X.L. Li, X.M. Sun, Y.D. Li, J. Phys. Chem. B 109 (2005) 12544.